2002-11-04

Attention: Nico Cortlever

Best regards, Helena

Soil improvement at Stockholm-Arlanda Airport

U. ERIKSSON, S. HANSBO and B.-A. TORSTENSSON

At Stockholm-Arlanda Airport a new, third runway is under construction. The project comprises a 2500 m long runway, new taxiways, areas for de-icing and surface water treatment, new public roads, bridges, a new traffic control tower, etc. The conditions at the site of the airport are difficult from a geotechnical standpoint and have necessitated different types of soil improvement techniques. Amongst these, vertical drainage in combination with preloading, consisting of 14–20 m of fill, has been used along the runway/taxiway over an area of 250 000 m^2 containing clay and organic deposits. In this paper, a description and theoretical analysis of the vertical-drain project are presented. The load of the fill has caused a relative compression of 22–29%, corresponding to total settlements of 1·6–2·6 m.

Une nouvelle et troisième piste d'atterrissage est en construction à l'aéroport de Stockholm. Le projet comprend une piste d'atterrissage d'une longueur de 2500 m, des nouvelles voies d'accès, des zones de dégivrage et de traitement des eaux superficielles, des nouvelles voies publiques, des ponts, une nouvelle tour de contrôle etc. Les conditions sur le site de l'aéroport sont compliquées du point de vue géotechnique et ont nécessité l'emploi de différentes techniques d'amélioration du sol. Entre autres, la technique de drainage vertical avec préchargement sous forme d'un remblai d'une hauteur de 14 à 20 m a été utilisée sur les surfaces d'atterrissage et d'accès qui couvrent 250 000 m^2 et dont le sous-sol consiste d'argiles molles et de dépots organiques. Une description et une analyse théorique du projet de drainage vertical sont présentées dan cet article. Le préchargement a entrainé une compression relative de 22 à 29%, correspondant à des tassements de 1,5 à 2,6 m.

Description of the Stockholm-Arlanda project

In a previous paper (Eriksson, 1997) a description was given of the soil stabilization measures started in the Stockholm-Arlanda project, including vertical drainage and preloading. The difficulties to be expected in the analysis of the consolidation process were discussed. The requirements placed on the completed project allowed a maximum settlement of 30 mm. The design of the vertical-drain project aimed at creating an effective preconsolidation pressure of at least 1·25 times the effective vertical pressure reached in the soil after completion of the project. This was done since, according to Scandinavian experience, an overconsolidation ratio OCR of 1·25 eliminates the risk of creep settlements after the primary consolidation period (Bjerrum, 1973). The drain spacing and the preloading conditions were selected in order to achieve 95% primary consolidation within twelve months of loading. In order to achieve this goal, preloading was carried out by means of 14–20 m of fill.

Owing to the uncertainties involved in the analysis of the final consolidation settlement, one year of loading could be expected to produce settlement values different from those predicted. This would lead to an unforeseen magnitude of the unloading required to reach the correct level of the runway/taxiway. As the overconsolidation ratio depends on the unloading carried out, the final design was made on the basis of the settlements and pore pressures observed during the construction period. In this way the necessary adjustments of the overload could be made in order to reach the acceptance criteria in due time (the observational method). In order to check the reliability of the settlement analysis, Asaoka's method of predicting the final primary consolidation settlement on the basis of settlement observations during the consolidation period was utilized.

At six sites of observation, settlement gauges and piezometers were installed in order to follow up the consolidation process in detail. Moreover, a large number of levelling marks were placed on top of the overload and followed in order to detect possible anomalies in the consolidation behaviour. Acceptance of the soil improvement works was based on the observations according to the following criteria:

- OCR $\geq$ 1·25 and $s = 0{\cdot}95 s_p$ at every site of observation (s_p = primary consolidation settlement under the overload)
- the settlements of the levelling marks should be approximately linear on a log-time scale
- the degree of primary consolidation $U \geq 95\%$ in the vicinity of the levelling marks
- the unloading after the preloading phase should amount to at least 25% of the overload.

Drain installation

Requirements

According to the design requirements, the drains had to be installed in an equilateral triangular pattern with a drain

(GI 089) Paper received 29 September 1999; accepted 15 December 1999

1365-781X

spacing of 0·9 m. Furthermore, depending on the large relative compression to be expected, the drains had to be capable of undergoing a vertical compression of the order of 35% without losing their function.

Type of vertical drains

The proven Mebradrain 88 was selected for the project (Fig. 1). This type of premanufactured drain, which has dimensions 4 × 100 mm, is furnished with a filter jacket of thermally bonded polypropene fabrics. The core of the drain, also made of polypropene, has a geometry which makes possible large vertical compression without substantial reduction of its water discharge capacity. The drains are delivered in rolls, each containing a length of 250 m.

Installation equipment

The installation of the drains was performed by means of a hydraulically operated drain rig (Fig. 2). Depending upon the depth of installation, this type of rig makes possible a production within the range of 6000–8000 m of drains per working day. Two drain rigs were utilized.

The installation of the drains was performed using a steel mandrel with dimensions 60 × 120 mm (Fig. 3). The size of the mandrel has been optimized with regard to requirements for mechanical strength and prevention of unnecessary disturbance of the subsoil. Before installation, rectangular anchor plates of steel were fixed to the tip of the drains to serve as anchors when the mandrel was withdrawn from the soil. The anchor plates also prevent soil from penetrating inside the mandrel during installation. If this happened there would be a risk that the drain might be withdrawn from the soil together with the mandrel. It is also practical to use the anchor plates for setting out the drain installation net.

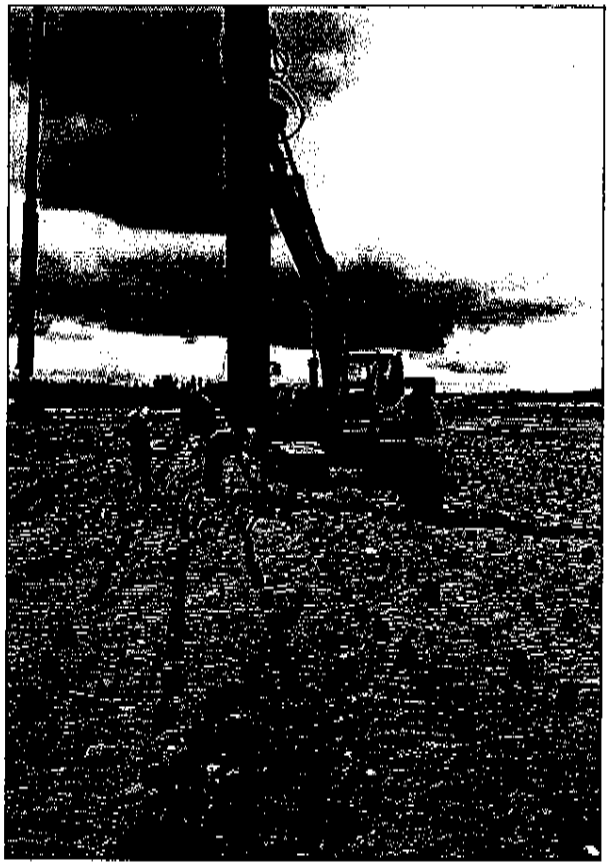

Fig. 2. Installation rig. Anchor plates, used for setting out the drain net, can be seen in the foreground

Soil and loading conditions at sites of observation

Three cases of observations will be presented, namely sites K, L and D. Sites K and L are situated along one of the new taxiways, where the soil consists of a comparatively thin organic layer underlain by clay with silt and sand seams. Site D is situated in a bog in the area of the new runway, where the soil consists of 2·3 m of peat underlain by gyttja (mud) and clay. The peat layer at site D was excavated before preloading.

The clay at sites K and L (Fig. 4) was medium to highly sensitive and normally consolidated, with a water content of mainly 60–90% and a liquid limit of 40–80%. The undrained shear strength was fairly constant, mainly about 7–9 kPa, irrespective of depth. The groundwater level was situated just below the ground level.

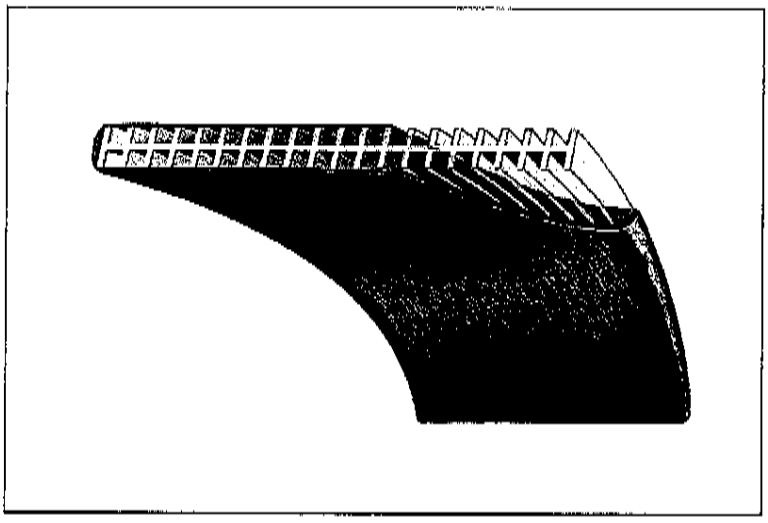

Fig. 1. Premanufactured drain, type Mebradrain 88

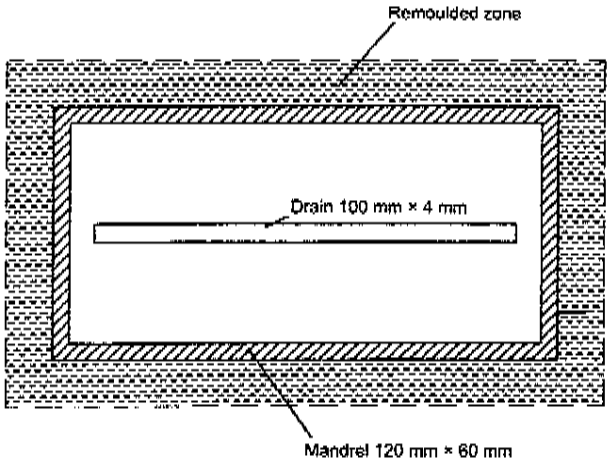

Fig. 3. Cross-sectional dimensions of the Mebradrain installed and of the mandrel utilized. The cross-sectional area of the remoulded zone indicated corresponds to the cross-sectional area of the mandrel (7200 mm²)

The clay at site D (Fig. 4) was medium to highly sensitive and normally consolidated, with a water content of 50–100% and a liquid limit of 40–80%. The mud at site D had a water content and a liquid limit of about 180%. The undrained shear strength was fairly constant, mainly about 6–14 kPa, irrespective of depth. The groundwater level was initially situated about 0·5 m below the ground level but was lowered 1·5 m when the peat was excavated and remained at that level during the whole preloading period.

At site K the load Δq consists of 19·5 m of till ($\gamma_{av.} = 20$ kN/m²), yielding $\Delta q = 390$ kN/m². At site L the load consists of 16·2 m of till, yielding $\Delta q = 325$ kN/m². At site D the load consists of 12·3 m of rock fill ($\gamma_{av.} = 16$ kN/m³) and 1·5 m of sand and gravel ($\gamma_{av.} = 19$ kN/m³). In the later case 2·3 m of peat ($\gamma_{av.} = 12$ kN/m³) was excavated and the groundwater level lowered 1·5 m. This yields $\Delta q = 215$ kN/m². The load at the various sites was placed stepwise (see Figs 7–9).

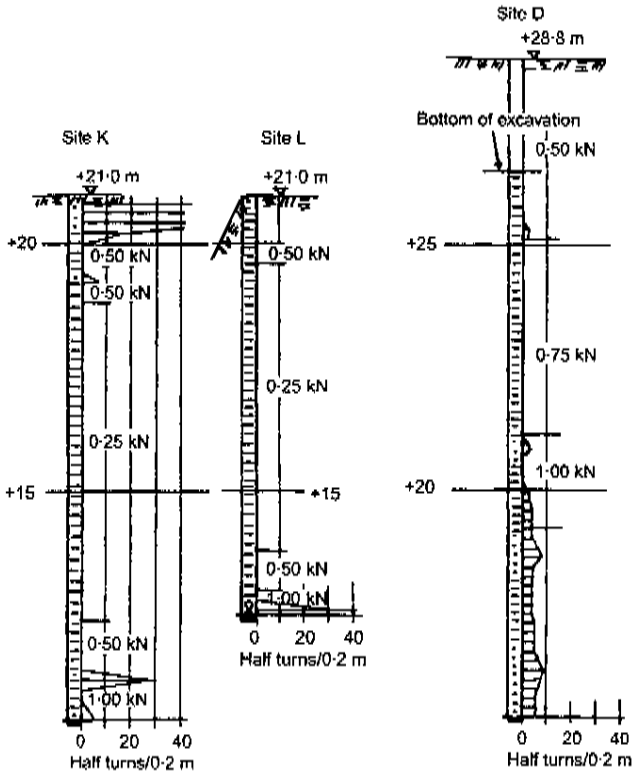

Fig. 4. Results of mechanized weight sounding at the sites of observation. The resistance is given as the smallest standard load for which the penetrometer sinks without rotation. For the highest load, 1 kN, the resistance is represented by the number of half turns required per 0·2 m of penetration

Settlement and excess-pore-pressure analysis

Primary-settlement analysis

In order to cope with the influence on the course of settlement of a time-consuming stepwise placement of the load, each break in the rate of loading can be analysed either on the basis of a direct use of oedometer curves or by the use of oedometer parameters (Fig. 5). In the latter case, the total primary settlement s caused by a load q on normally consolidated clay can be obtained from the relation

$$s = \sum_{j=1}^{m} \Delta h_j \times \left[\frac{\sigma'_{Lj} - \sigma'_{cj}}{M_{Lj}} + \frac{1}{M'_j} \ln\left(1 + \frac{M'_j[q - (\sigma'_{Lj} - \sigma'_{cj}) - s(\gamma - \gamma')]}{M_{Lj}}\right)\right] \quad (1)$$

where Δh_j is the thickness of layer j, $M_j = \Delta\sigma'_j/\Delta\varepsilon_j$ is the compression modulus of layer j determined by oedometer tests, $M'_j = \Delta M_j/\Delta\sigma'_j$ (see Fig. 5), $q \geq \sigma'_{Lj} - \sigma'_{cj}$, σ'_{cj} is the preconsolidation pressure of layer j, $\sigma'_{Lj} - \sigma'_{cj}$ is the stress interval above the preconsolidation pressure with constant compression modulus M_{Lj}, m is the number of layers and $s(\gamma - \gamma')$ represents the reduction in load caused by the fact that part of the load becomes submerged in the course of settlement. If $q < \sigma'_{Lj} - \sigma'_{cj}$ the relation becomes equal to

$$s = \sum_{j=1}^{m} \frac{\Delta h_j q}{M_{Lj}} \quad (2)$$

From the results of the oedometer tests, the parameters and consequent consolidation settlements listed in Tables 1–3 were obtained. At site D the total primary settlement caused by the placement of the drainage layer, excavation of the peat layer and groundwater lowering (load increase $q = 16$ kN/m²) amounts to 0·43 m.

The settlement values calculated on the basis of the oedometer tests were compared with those determined by Asaoka's method. This results in the correlation

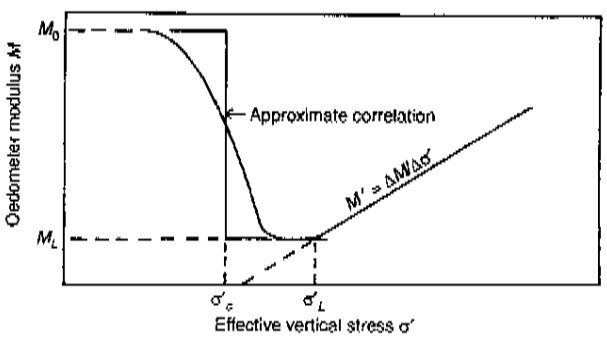

Fig. 5. Oedometer parameters used in the settlement analysis

Table 1. Parameters and calculated consolidation settlements for site K

Depth: m	M_{ij}: kPa	M'_j	$\sigma'_{ij} - \sigma'_{dj}$: kPa	Δh_j: m	Load step: kN/m²	Settlement: m
2	80	12·9	9	2·5	0–80	1·8
4	165	19·3	12	2·0	80–215	0·7
6	188	15·3	21	2·0	215–390	0·4
8	279	17·5	20	2·5	0–390	2·9

Table 2. Parameters and calculated consolidation settlements for site L

Depth: m	M_{ij}: kPa	M'_j	$\sigma'_{ij} - \sigma'_{dj}$: kPa	Δh_j: m	Load step: kN/m²	Settlement: m
2	228	11·9	11	2·0	0–80	1·25
4	225	17·1	16	2·25	80–325	0·7
6·5	260	18·3	22	1·75	0–325	1·85
7·5	575	24·4	40	0·8		

Table 3. Parameters and calculated consolidation settlements for site D

Depth: m	M_{ij}: kPa	M'_j	$\sigma'_{ij} - \sigma'_{dj}$: kPa	Δh_j: m	Load step: kN/m²	Settlement: m
3	228	12·9	9	1·8	0–80	1·25
5	225	19·3	12	1·5	80–145	0·35
6	260	15·3	21	1·0	145–195	0·15
7	575	17·5	20	1·0	195–215	0·10
8	288	16·6	29	3·0	0–215	185

$s_i = 0{\cdot}5905 + 0{\cdot}7755 s_{i-1}$ at site K, from which $s_p = 2{\cdot}63$ m, and $s_i = 0{\cdot}2488 + 0{\cdot}8487 s_{i-1}$ at site L, from which $s_p = 1{\cdot}64$ m. The correlation obtained in the case of site D is $s_i = 1{\cdot}0414 + 0{\cdot}5022 s_{i-1}$, from which $s_p = 2{\cdot}09$ m.

As can be seen, the primary settlements evaluated on the basis of oedometer tests are both higher and lower than those obtained by Asaoka's method. The discrepancy can be explained by the fact that the oedometer tests were carried out on samples taken as far as 25–175 m away from the points of settlement observation. In order to adjust the settlement values calculated from the oedometer tests, the settlements obtained for the various load steps were adjusted by multiplication by a factor obtained by dividing the final settlement values obtained by Asaoka's method by the final settlement values evaluated on the basis of the oedometer tests. By doing this, the settlement values in Tables 1–3 are changed to the values in Table 4.

Analysis of consolidation process

The analysis of the consolidation process, carried out on the assumption of both Darcian and non-Darcian flow, was presented by the senior author (Hansbo, 1997). In a case like this, where the hydraulic gradients created by the loading operation are exceptionally high (up to about 100), the analysis of the consolidation process on the basis of Darcian flow gives equally good agreement with real behaviour as an analysis based on non-Darcian flow (as defined by Hansbo (1960, 1997)). Therefore, this analysis will be restricted to using Darcian flow as a basis for the consolidation analysis. Taking into account both vertical and radial escape of pore water, the average degree of consolidation is obtained from the relation

$$\overline{U}_{av} = 1 - \left(1 - \frac{2}{l}\sqrt{\frac{c_v t}{\pi}}\right) \exp\left(-\frac{8 c_h t}{\mu_{av} D^2}\right) \qquad (3)$$

where $\mu_{av} = \ln(D/d_s) + (k_h/k_s)\ln(d_s/d_w) - 3/4 + 2k_h\pi l^2/3q_w$, c_v is the coefficient of consolidation for vertical pore water flow, c_h is the coefficient of consolidation for horizontal pore water flow, l is the full or half length of the drain, if closed or open, respectively, at bottom, D is the diameter of the soil cylinder dewatered by a drain, d_s is the diameter of the zone of smear, d_w is the drain diameter, k_h is the permeability in the horizontal direction in undisturbed soil, k_s is the permeability in the horizontal direction in the zone of smear and, q_w is the specific discharge capacity of the drain (for vertical hydraulic gradient $i = 1$) (see Fig. 6).

Diameter d_w

A band-shaped prefabricated drain can be assumed to correspond to a cylindrical drain having a circumference

Table 4. Adjusted settlement values (see text)

Site K		Site L		Site D	
Load step: kN/m²	Settlement: m	Load step: kN/m²	Settlement: m	Load step: kN/m²	Settlement: m
1: 0–80	1·63	1: 0–80	1·02	1: 0–16	0·48
2: 80–215	0·64	2: 80–325	0·62	2: 16–80	0·93
3: 215–390	0·36			3: 80–145	0·40
				4: 145–195	0·17
				5: 195–215	0·11
0–390	2·63	0–325	1·64	0–215	2·09

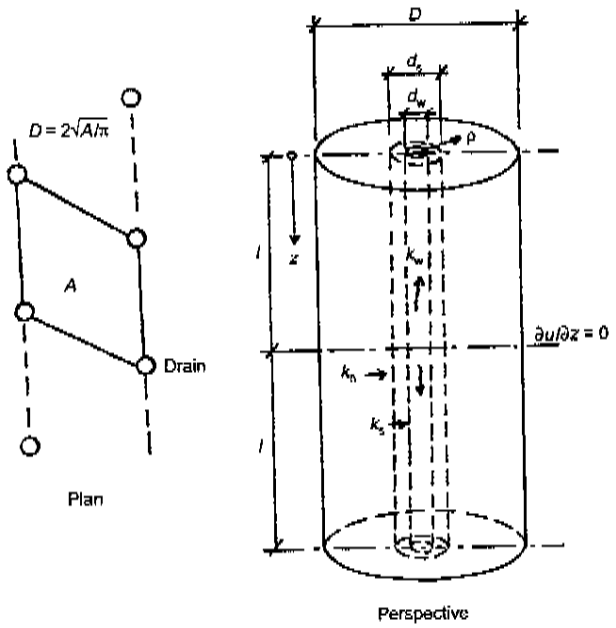

Fig. 6. Terms used in the analysis of vertical drains. Upper and lower surfaces drained. l = full or half length of drain if closed or open, respectively, at bottom; D = diameter of soil cylinder dewatered by a drain; d_s = diameter of zone of smear; d_w = drain diameter; k_h = permeability in the horizontal direction in undisturbed soil; k_s = permeability in the horizontal direction in the zone of smear; k_w = permeability in the longitudinal direction of the drain

equal to that of the band-shaped drain (Hansbo, 1979). Thus, the diameter d_w of the Mebradrain 88 installed in this case can be assumed equal to 66 mm.

Diameter d_s

The installation of the drains will cause a zone of smear (with more or less remoulded soil) around the drains (Chai *et al.*, 1997). The extent of the zone of smear and the disturbance effects depend on the type of soil and the geometrical dimensions of the installation mandrel. Remoulding will take place inside a volume equal to the volume displaced by the mandrel (Torstensson, 1973); see Fig. 3. Outside the remoulded zone, disturbance of the subsoil will also occur owing to distortion. The extent of the zone of distortion is a function of the stiffness of the subsoil. The stiffer the soil, the larger the zone of influence, and vice versa. The extent of the zone of disturbance (smear) in the case of displacement-type circular drains has been assumed equal to about two times the diameter of the drains (Holtz and Holm, 1973; Akagi, 1976; Bergado *et al.*, 1992). Recent investigations on a laboratory scale indicate that this assumption is too conservative and that a better estimate is 1·6 times the diameter of the drain (Onoue *et al.*, 1991; Hird and Moseley, 1997). Accordingly, the cross-sectional area of the zone of smear can be set equal to $1{\cdot}6^2$ times the cross-sectional area of the mandrel, in the present case corresponding to a diameter of the zone of smear of 150 mm.

Consolidation characteristics

At sites K and L the coefficient of consolidation c_v, according to the oedometer tests, varies from about 0·2–0·3 m^2/year at the preconsolidation pressure to about 0·5–1·0 m^2/year (maximum 2·5 m^2/year) at the end of primary compression under the maximum load applied (300 kN/m^2). At site D the corresponding values vary from about 0·15–0·3 m^2/year at the preconsolidation pressure to about 0·3–1·3 m^2/year at the end of primary compression under the maximum load applied (300 kN/m^2).

Theoretical versus observed course of settlement

The following assumptions were applied in the analysis: $k_h/k_s = c_h/c_v = 3$; $l = 4{\cdot}5$ m at sites K and D; $l = 4$ m at site L. The values of c_h to be used in the analysis were found by trial and error (observational method).

The loading conditions and the settlement observations at sites K, L and D are shown in Figs 7–9. In these cases, where a great deal of the consolidation process takes place during the loading period, the settlement curves have to be adjusted for the rate of loading, for instance according to the well-known graphical procedure suggested by Terzaghi.

Site K (Fig. 7). The best fit between theory and observations is obtained for $c_h = 2{\cdot}25$ m^2/year. Inserting the

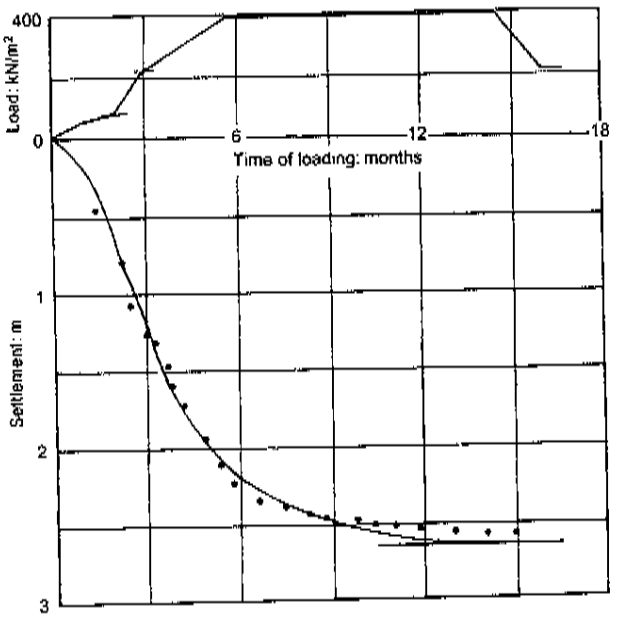

Fig. 7. Results of settlement observations at site K compared with results of theoretical analysis

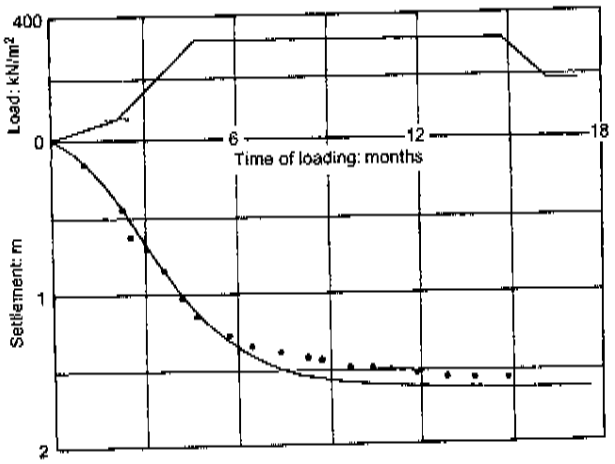

Fig. 8. Results of settlement observations at site L compared with results of theoretical analysis

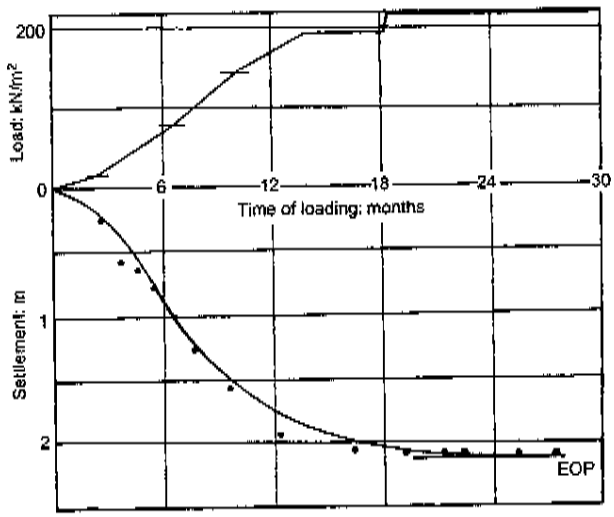

Fig. 9. Results of settlement observations at site D compared with results of theoretical analysis. EOP, end of primary settlement

consolidation time $t_1 = 1$ month (the length of time that corresponds to the full loading condition in load step 1), we find $\overline{U}_1 = 0{\cdot}42$ at the completion of load step 1, and, consequently, $s = 0{\cdot}42 \times 1{\cdot}63 = 0{\cdot}69$ m. At the completion of load step 2 ($t_1 = 2$ months and $t_2 = 0{\cdot}5$ months) we find $\overline{U}_1 = 0{\cdot}65$ and $\overline{U}_2 = 0{\cdot}25$, whence $s = 0{\cdot}65 \times 1{\cdot}63 + 0{\cdot}25 \times 0{\cdot}63 = 1{\cdot}22$ m. Finally, at the completion of load step 3 ($t_1 = 4{\cdot}5$ months, $t_2 = 3$ months and $t_3 = 1{\cdot}25$ months) we find $\overline{U}_1 = 0{\cdot}90$, $\overline{U}_2 = 0{\cdot}79$ and $\overline{U}_3 = 0{\cdot}49$, i.e. $s = 0{\cdot}90 \times 1{\cdot}63 + 0{\cdot}79 \times 0{\cdot}63 + 0{\cdot}49 \times 0{\cdot}36 = 2{\cdot}15$ m. Three months later we find $\overline{U}_1 = 0{\cdot}98$, $\overline{U}_2 = 0{\cdot}95$ and $\overline{U}_3 = 0{\cdot}89$, i.e. $s = 0{\cdot}98 \times 1{\cdot}63 + 0{\cdot}95 \times 0{\cdot}63 + 0{\cdot}89 \times 0{\cdot}36 = 2{\cdot}52$ m. Another three months later we find $\overline{U}_1 = 0{\cdot}995$, $\overline{U}_2 = 0{\cdot}99$ and $\overline{U}_3 = 0{\cdot}98$, i.e. $s = 2{\cdot}60$ m.

Site L (Fig. 8). Here also, the best fit between theory and observations is obtained for $c_h = 2{\cdot}25$ m²/year. Inserting the consolidation time $t_1 = 1$ month (the length of time that corresponds to the full loading condition in load step 1), we find $\overline{U}_1 = 0{\cdot}42$ at the completion of load step 1, and, consequently, $s = 0{\cdot}42 \times 1{\cdot}02 = 0{\cdot}43$ m. At the completion of load step 2 ($t_1 = 3{\cdot}5$ months and $t_2 = 1{\cdot}25$ months) we find $\overline{U}_1 = 0{\cdot}83$ and $\overline{U}_2 = 0{\cdot}48$, whence $s = 0{\cdot}83 \times 1{\cdot}02 + 0{\cdot}48 \times 0{\cdot}62 = 1{\cdot}15$ m. Three months later we find $\overline{U}_1 = 0{\cdot}96$, $\overline{U}_2 = 0{\cdot}88$, whence $s = 1{\cdot}53$ m. Another three months later we find $\overline{U}_1 = 0{\cdot}99$, $\overline{U}_2 = 0{\cdot}97$, i.e. $s = 1{\cdot}61$ m.

Site D (Fig. 9). The best fit between theory and observations is obtained for $c_h = 1{\cdot}75$ m²/year. Inserting the consolidation time $t_1 = 1$ month (the length of time that corresponds to the full loading condition during the placement of the drainage layer, load step 1), we find $\overline{U}_1 = 0{\cdot}35$, whence $s = 0{\cdot}35 \times 0{\cdot}44 = 0{\cdot}15$ m. The length of time required for the placement of load step 2 was 4·5 months. Thus, at the completion of load step 2 ($t_1 = 5{\cdot}5$ months and $t_2 = 2{\cdot}25$ months) we find $\overline{U}_1 = 0{\cdot}89$ and $\overline{U}_2 = 0{\cdot}63$, whence $s = 0{\cdot}89 \times 0{\cdot}44 + 0{\cdot}61 \times 1{\cdot}05 = 1{\cdot}03$ m. At the completion of load step 3 ($t_1 = 7$ months and $t_2 = 5{\cdot}25$ months and $t_3 = 1{\cdot}5$ months) we find $\overline{U}_1 = 0{\cdot}94$, $\overline{U}_2 = 0{\cdot}88$ and $\overline{U}_3 = 0{\cdot}47$, i.e. $s = 0{\cdot}94 \times 0{\cdot}44 + 0{\cdot}88 \times 1{\cdot}05 + 0{\cdot}47 \times 0{\cdot}35 = 1{\cdot}50$ m. At the completion of load step 4 ($t_1 = 11$ months, $t_2 = 9{\cdot}25$ months, $t_3 = 5{\cdot}5$ months and $t_4 = 2$ months) we find $\overline{U}_1 = 0{\cdot}99$, $\overline{U}_2 = 0{\cdot}97$, $\overline{U}_3 = 0{\cdot}89$ and $\overline{U}_4 = 0{\cdot}57$, i.e. $s = 0{\cdot}99 \times 0{\cdot}44 + 0{\cdot}98 \times 1{\cdot}05 + 0{\cdot}89 \times 0{\cdot}35 + 0{\cdot}58 \times 0{\cdot}20 = 1{\cdot}88$ m. When load step 5 is applied we have $\overline{U}_1 = \overline{U}_2 = \overline{U}_3 = 1{\cdot}0$ and $\overline{U}_4 = 0{\cdot}93$, from which $s = 1{\cdot}0 \times 1{\cdot}84 + 0{\cdot}93 \times 0{\cdot}20 = 2{\cdot}03$ m. Three months later we find $\overline{U}_1 = \overline{U}_2 = \overline{U}_3 = 1{\cdot}0$, $\overline{U}_4 = 0{\cdot}98$ and $\overline{U}_5 = 0{\cdot}72$, i.e. $s = 1{\cdot}0 \times 1{\cdot}84 + 0{\cdot}98 \times 0{\cdot}20 + 0{\cdot}72 \times 0{\cdot}05 = 2{\cdot}07$ m.

As can be seen from Figs 7–9, the agreement between the theoretical and the observed course of primary consolidation settlement is quite good provided that the analysis is based upon the final consolidation settlement obtained by Asaoka's method.

Theoretical versus observed excess-pore-pressure dissipation

According to Skempton (1954), the excess pore pressure Δu caused by loading of water-saturated clay can be expressed by the relation

$$\Delta u = \Delta h \gamma_w = A \Delta\sigma_1 + (1 - A)\Delta\sigma_3 \tag{4}$$

where $\Delta\sigma_1$ is the increase in the total major principal stress due to loading, $\Delta\sigma_3$ is the increase in the total minor principal stress due to loading and A is the pore pressure coefficient, the value of which depends upon the clay properties, the preloading history and the magnitude of the load increase above the preconsolidation pressure.

In our case, where the clay is medium to highly sensitive and normally consolidated and the loading conditions are extreme, the value of A is certainly above 1·0, most probably around 1·1–1·3 (Hansbo, 1994). The stress increase in the middle of the clay layer at the various sites is $\Delta\sigma_1 = \Delta q$ and $\Delta\sigma_3 = 0{\cdot}9\,\Delta q$ according to the theory of elasticity. Choosing $A = 1{\cdot}2$, we find $\Delta u_0 = \Delta h_0 \gamma_w = 1{\cdot}02\,\Delta q$, i.e. $\Delta h_0 = 0{\cdot}104\,\Delta q$.

Ignoring the influence of one-dimensional vertical drainage, the excess pore pressure Δu outside the zone of smear becomes equal to (Hansbo, 1981)

$$\Delta u = \frac{\gamma_w}{8k_h}\frac{\partial\varepsilon}{\partial t}\left[D^2 \ln\frac{2\rho}{d_s} - \frac{4\rho^2 - d_s^2}{2} + \frac{k_h}{k_s}\left(D^2 \ln\frac{d_s}{d_w} - \frac{d_s^2 - d_w^2}{2}\right) + \frac{k_h}{q_w}\pi z(2l - z)(D^2 - d_w^2)\right] \tag{5}$$

where ρ is the radius vector ($D/2 \geq \rho \geq d_s/2$) and D, d_w, d_s, k_h, k_s, l, z and q_w are as previously defined.

Inserting

$$\frac{\gamma_w}{8k_h}\frac{\partial\varepsilon}{\partial t} = -\frac{1}{8c_h}\frac{\partial\overline{u}}{\partial t} = \frac{\Delta u_0}{8c_h}\frac{\partial\overline{U}_h}{\partial t} \tag{6}$$

$$\overline{U}_h = 1 - \exp\left(-\frac{8c_h t}{\mu D^2}\right) \tag{7}$$

we find

$$\frac{\gamma_w}{8k_h}\frac{\partial\varepsilon}{\partial t} = \frac{\Delta u_0}{\mu D^2}(1 - \overline{U}_h) \tag{8}$$

Ignoring well resistance, which in our case is justified, the piezometric head $\Delta h = \Delta u/\gamma_w$ becomes equal to

$$\Delta h = \frac{\Delta h_0}{\mu D^2}(1 - \overline{U}_h) \times \left[D^2 \ln\frac{2\rho}{d_s} - \frac{4\rho^2 - d_s^2}{2} + \frac{k_h}{k_s}\left(D^2 \ln\frac{d_s}{d_w} - \frac{d_s^2 - d_w^2}{2}\right)\right] \tag{9}$$

where $\mu = \ln(D/d_s) + (k_h/k_s)\ln(d_s/d_w) - 3/4$.

In our case the piezometers were placed inside concrete tubes with an outer diameter of 1 m before the installation of the drains. The concrete tubes were aimed at protecting the piezometers during the filling operation. The existence of these tubes created an obstacle to keeping up the intended

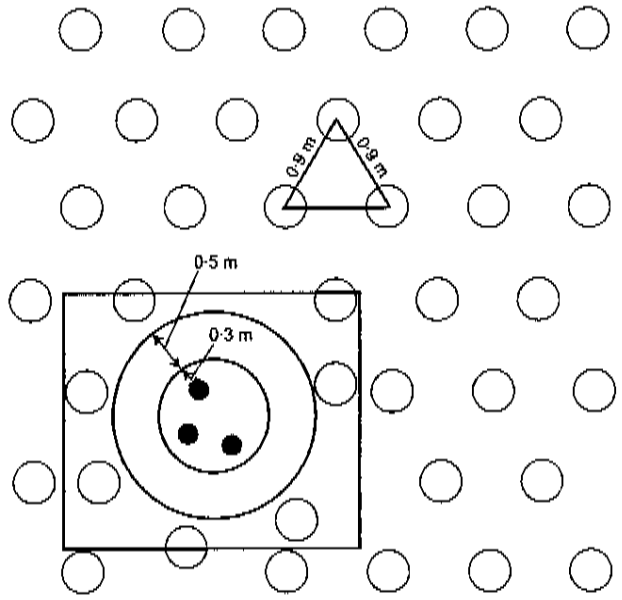

Fig. 10. Example of installation of drains (open circles) around piezometers (filled circles). The closest distance between a drain and a piezometer is about 0·9 m. Within the area of the rectangle the average area covered by each drain is 1·4 m², which corresponds to an average D value of 1·335 m instead of the normal D value of 0·945 m

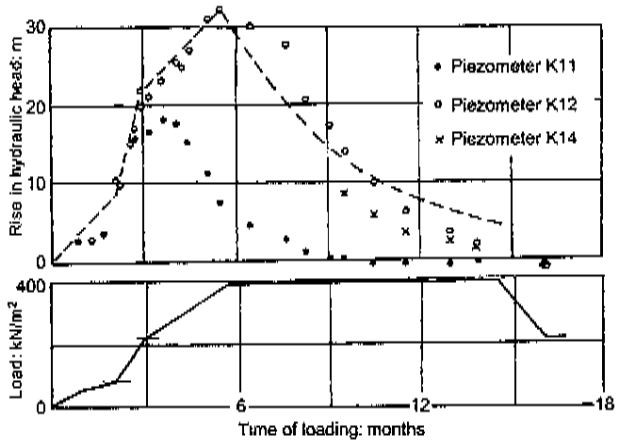

Fig. 11. Results of pore pressure observations at site K compared with results of theoretical analysis. Piezometers placed at the following levels (level of original ground surface +21·0 m): K11, +17·0 m; K12, +15·0 m; K14 (after 10 months of loading), +14·3 m.

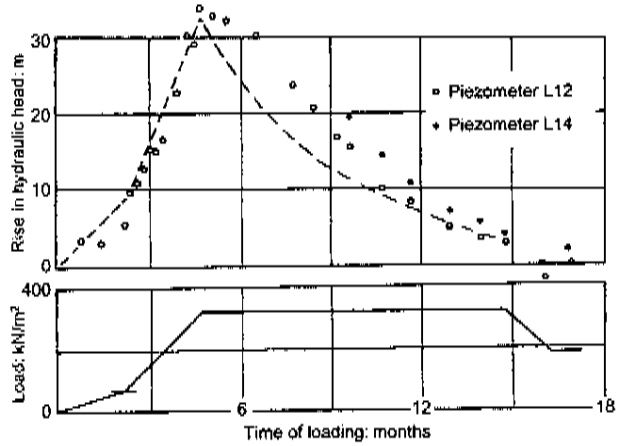

Fig. 12. Results of pore pressure observations at site L compared with results of theoretical analysis. Piezometers placed at the following levels (level of original ground surface +21·0 m): L12, +16·0 m; L14, +14·0 m

drain pattern (Fig. 10). Thus, the distance from a piezometer to the nearest drain can be estimated as 0·9 m. The average D value in the vicinity of a piezometer can be estimated as 1·335 m instead of the normal value of 0·945 m. Assuming that the piezometer is placed in the centre between the drains, we have $\rho/D = 0{\cdot}5$, corresponding to $D = 1{\cdot}8$ m. For $\overline{U} = 0$ we then have $\Delta h = 1{\cdot}06 \times 0{\cdot}104\,\Delta q = 0{\cdot}11\,\Delta q$. (The same result is obtained for $D = 1{\cdot}335$ or 0·945 m.) When dealing with the excess-pore-pressure dissipation, the excess pore pressure developed during the placement of each load step is assumed to correspond to the total load increase (no reduction of the pore pressure is caused during the placement of the load step). This can be justified by the dynamic disturbance effects caused by the filling operation. The time of consolidation is, therefore, chosen with reference to the time when the filling operation in a load step is completed. The choice of the D value in the analysis is somewhat intricate with regard to the placement of the drains around the piezometers. The best estimate seems to be to apply the average D value in the vicinity of a piezometer, namely $D = 1{\cdot}335$ m.

Site K (Fig. 11). Proceeding as described above and taking into account only the effect of the drains ($c_v = 0$), we find, at the completion of loading, $\Delta h = 0{\cdot}11 \times 80 = 8{\cdot}8$ m. At the completion of load step 2 we have $t_1 = 1$ month, which yields $\overline{U}_1 = 0{\cdot}19$. Hence $\Delta h = 0{\cdot}81 \times 8{\cdot}8 + 0{\cdot}11 \times 135 = 22{\cdot}0$ m. At the completion of load step 3 we have $t_1 = 3{\cdot}5$ months and $t_2 = 2{\cdot}5$ months, from which $\overline{U}_1 = 0{\cdot}53$ and $\overline{U}_2 = 0{\cdot}42$; from this we obtain $\Delta h = 0{\cdot}47 \times 8{\cdot}8 + 0{\cdot}58 \times 0{\cdot}11 \times 135 + 0{\cdot}11 \times 175 = 32{\cdot}0$ m. An easier way of finding the value of Δh, which applied in the following, is to start the analysis from the time when load step 2 is completed; this yields the same result, $\Delta h = 0{\cdot}58 \times 22{\cdot}0 + 0{\cdot}11 \times 175 = 32{\cdot}0$ m. Three months later we have $\overline{U}_3 = 0{\cdot}48$, whence $\Delta h = 0{\cdot}52 \times 32{\cdot}0 = 16{\cdot}7$ m, and another three months later, $\overline{U}_2 = 0{\cdot}73$, i.e. $\Delta h = 0{\cdot}27 \times 32{\cdot}0 = 8{\cdot}7$ m.

Site L (Fig. 12). At the completion of load step 1, $\Delta h = 0{\cdot}11 \times 80 = 8{\cdot}8$ m. At the completion of load step 2 we have $t_1 = 2{\cdot}5$ months, which yields $\overline{U}_1 = 0{\cdot}42$. Hence $\Delta h = 0{\cdot}58 \times 8{\cdot}8 + 0{\cdot}11 \times 245 = 32{\cdot}1$ m. Four months later we have $\overline{U}_2 = 0{\cdot}58$, whence $\Delta h = 0{\cdot}42 \times 32{\cdot}1 = 13{\cdot}5$ m, and another four months later $\overline{U}_2 = 0{\cdot}82$, whence $\Delta h = 0{\cdot}18 \times 32{\cdot}9 = 5{\cdot}7$ m.

Site D (Fig. 13). At the completion of load step 1, $\Delta h = 0{\cdot}11 \times 16 = 1{\cdot}7$ m. At the completion of load step 2 we have $t_1 = 4{\cdot}5$ months, from which $\overline{U}_1 = 0{\cdot}53$, yielding $\Delta h = 0{\cdot}47 \times 1{\cdot}7 + 0{\cdot}11 \times 64 = 7{\cdot}8$ m. At the completion of load step 3 ($t_2 = 3$ months) we find $\overline{U}_2 = 0{\cdot}40$, and hence $\Delta h = 0{\cdot}60 \times 7{\cdot}8 + 0{\cdot}11 \times 65 = 11{\cdot}9$ m. At the completion of load step 4 ($t_3 = 3$ months) we have $\overline{U}_3 = 0{\cdot}40$, whence $\Delta h = 0{\cdot}60 \times 11{\cdot}9 + 0{\cdot}11 \times 50 = 12{\cdot}6$ m. At the beginning and completion of load step 5 we find ($t_4 = 4$ and 4·5 months, respectively) $\overline{U}_4 = 0{\cdot}49$ and 0·53, respectively, from which $\Delta h = 0{\cdot}51 \times 12{\cdot}6 = 6{\cdot}4$ m and $\Delta h = 0{\cdot}47 \times 12{\cdot}6 + 0{\cdot}11 \times 20 = 8{\cdot}1$ m, respectively. Four months later we have $\overline{U}_5 = 0{\cdot}49$, whence $\Delta h = 0{\cdot}51 \times 8{\cdot}1 = 4{\cdot}1$ m, and another four months later $\overline{U}_5 = 0{\cdot}74$, whence $\Delta h = 0{\cdot}26 \times 8{\cdot}1 = 2{\cdot}1$ m.

Considering the difficulties in selecting the correct input value of D in the analysis, an acceptable agreement is obtained betwen the theoretical course of excess-pore-pressure dissipation and the observations.

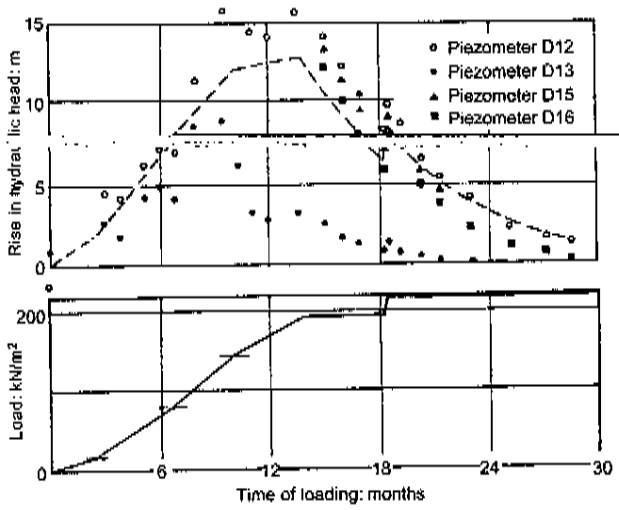

Fig. 13. Results of pore pressure observations at site D compared with results of theoretical analysis. Piezometers placed at the following levels (level of original ground surface +28·8 m): D12, +23·3 m (+22·0 m after 14 months of loading); D13, +20·5 m (+19·5 m after 14 months of loading); D15, +22·5 m; D16, +20·5 m

Discussion

The agreement between theory and practice depends very much on the correctness of the estimate of final primary consolidation settlement. In our case, the estimate based on oedometer tests leads to both larger and smaller primary settlements than those evaluated by Asaoka's method. The latter method, which cannot be applied until a great deal of the consolidation process has taken place, is a valuable tool in the observational method. The agreement between the observations and the theoretical course of settlement (with consolidation parameters adjusted to get the best overall fit) is quite good.

The excess pore pressure created in the loading process is considerably larger than can be estimated according to consolidation theory. The reason seems to be the dynamic influence of the loading operation. The theoretical evaluation performed in our case disregards the effect of time on the consolidation process during the placement itself of each load step. After the loading operation is terminated, the agreement between the theoretical and the observed excess-pore-pressure dissipation is acceptable.

One may question whether the selected parameters represent the truth in the consolidation analysis. The same results could be obtained by choosing, for instance, $d_w = 0{\cdot}19$ m (corresponding to a cross-sectional area of the zone of smear of 2^2 instead of $1{\cdot}6^2$ times the cross-sectional area of the mandrel), and $k_h/k_s = c_h/c_v = 6$, $c_h = 4{\cdot}5$ m^2/year (sites K and L) and $3{\cdot}5$ m^2/year (site D). In both cases the c_v value will be the same, $0{\cdot}75$ m^2/year (sites K and L) and $0{\cdot}58$ m^2/year (site D). In our case, the chosen parameters seem more realistic than those exemplified above. The reason why the c_v values can be chosen this high is most probably due to the unusually large size of the overload, equal to or even higher than the maximum load applied in the oedometer tests. As can be seen from the oedometer tests, the c_v value increases during the consolidation process: the higher the stress increase, the larger the c_v value. This may be the explanation of the fact that the excess-pore-pressure decrease at the end of the consolidation process is larger in reality than in theory (the c_v value was set equal to zero in the analysis).

Comparison between the rate of settlement and the rate of excess-pore-pressure dissipation shows discrepancies because of the fact that the drain pattern around the piezometers differs from the normal one. In our case, this was caused by the fact that the piezometers were installed before the drains, inside tubes that created an obstacle to the installation of drains in the normal pattern. Therefore it is necessary to apply a value of D in the analysis of excess-pore-pressure dissipation different from the value applied in the settlement analysis.

Although settlement may seem of greater interest than pore pressure, it is important that pore pressure is followed to ensure that the overload, if any, is not removed too early. A decision based solely on settlement measurements may be misleading since a slow rate of settlement may depend on a slow rate of excess-pore-pressure dissipation. In this case pore pressure observations were required in order to guarantee that the preconsolidation stress in the soil, after completion of the project, would exceed the effective vertical pressure in the soil by 25%.

References

Akagi T. (1976) *Effect of Displacement Type Sand Drains on Strength and Compressibility of Soft Clays*. Doctoral thesis, University of Tokyo.

Bergado D. T., Akasami H., Alfaro M. C. and Balasubramaniam A. S. (1992) Smear effects of vertical drains on soft Bangkok clay. *Journal of Geotechnical Engineering*, **117**, No. 10, 1509–1530.

Bjerrum L. (1973) Problems of soil mechanics and construction on soft clays and structurally unstable soils (collapsible, expansive and others). *Proceedings of the 7th International Conference on Soil Mechanics and Foundation Engineering, Moscow*, 3.

Eriksson U. (1997) Active design of preloading in combination with vertical drains. *Proceedings of the 14th International Conference on Soil Mechanics and Foundation Engineering, Hamburg*, 1, 477–480.

Chai J. C., Miura N. and Sakajo S. (1997) A theoretical study on smear effect around vertical drain. *Proceedings of the 14th International Conference on Soil Mechanics and Foundation Engineering, Hamburg*, 3, 1581–1584.

Hansbo S. (1960) *Consolidation of Clay, with Special Reference to Influence of Vertical Drains*. Swedish Geotechnical Institute, Proceeding No. 18. Doctoral thesis, Chalmers University of Technology, Gothenburg.

Hansbo S. (1979) Consolidation of clay by band-shaped prefabricated drains. *Ground Engineering*, **12**, No. 5, 16–25.

Hansbo S. (1981) Consolidation of fine-grained soils by prefabricated drains. *Proceedings of the 10th International Conference on Soil Mechanics and Foundation Engineering, Stockholm*, 3, 677–682.

Hansbo S. (1994) *Foundation Engineering*. Elsevier, Amsterdam.

Hansbo S. (1997) Aspects of vertical drain design—Darcian or non-Darcian flow. *Géotechnique*, **47**, No. 5, 983–992.

Hird C. C. and Moseley V. J. (1997) *Model Study of Smear Around Vertical Drains in Layered Soil*. Department of Civil and Structural Engineering, University of Sheffield.

Holtz R. D. and Holm G. (1973) Excavation and sampling around some drains at Skå-Edeby. *Proceedings of the Nordic Geotechnical Meeting*. Norwegian Geotechnical Institute, Oslo, pp. 79–85.

Onoue A., Ting N., Germaine J. T. and Whitman R. V. (1991) Permeability of disturbed zone and around vertical drains. American Society of Civil Engineers, New York, *Geotechnical Special Publication 27*, pp. 879–890.

Skempton (1954) The pore pressure coefficients A and B. *Géotechnique*, **4**, No. 4.

Torstensson B.-A. (1973) *Kohesionspålar i lös lera* [Behaviour of friction piles in soft clay]. Doctoral thesis, Chalmers University of Technology, Gothenburg.

Discussion contributions on this paper should reach the secretary by 31 August 2000